Surgical Endoscopy (2019) 33:2802–2811
https://doi.org/10.1007/s00464-018-6571-8

Ultrasound shear wave elastography effectively predicts integrity of ventral hernia repair using acellular dermal matrix augmented with platelet-rich plasma (PRP)

Jeffrey L. Van Eps[1,2] · Anuj Chaudhry[3] · Joseph S. Fernandez-Moure[1,2] · Christian Boada[2,4] · Vishwanath Chegireddy[1] · Fernando J. Cabrera[2] · Songyuan Tang[3] · Ennio Tasciotti[2] · Raffaella Righetti[5]

Received: 31 May 2018 / Accepted: 1 November 2018 / Published online: 13 December 2018
© Springer Science+Business Media, LLC, part of Springer Nature 2018

Abstract

Background Complications of ventral hernia repair (VHR) may be investigated by computed tomography or ultrasound (US) but neither modality gives a quantifiable metric of repair quality short of identifying hernia recurrence. Platelet-rich plasma (PRP), a growth factor-rich autologous blood product, has been shown to improve incorporation of native tissue with bioprosthetics. In this study, we investigate the effect of PRP on the incorporation and mechanical integrity of a non-crosslinked porcine acellular dermal matrix (pADM) in a rodent model of VHR and the correlative ability of ultrasound shear wave elastography (US-SWE) to assess repair quality.

Methods PRP was isolated from whole blood of Lewis rats. Twenty-eight Lewis rats underwent chronic VHR using either pADM alone or augmented with autologous PRP prior to non-invasive imaging assessment and specimen harvest at either 3 or 6 months. US-SWE was performed to estimate the Young's modulus prior to histological assessment and data from PRP-treated rodents were compared to controls.

Results Implanted pADM was easily distinguishable by US-SWE imaging in all cases analyzed in this study. The mean Young's modulus measured was 1.78 times and 2.54 times higher in PRP-treated samples versus control at 3-month and 6-month time points respectively ($p < 0.05$). At 3 months, qualitative and quantitative histology revealed decreased inflammation and improved incorporation in PRP-treated samples along the implant/abdominal wall interface. At 6 months, the PRP cohort had no hernia recurrence and preserved ADM integrity from immunologic degradation, while all control animals suffered hernia recurrence (4/6) or extreme ADM thinning (2/6).

Conclusion This study confirms both the efficacy of PRP in augmenting VHR using pADM, as well as the reliability of US-SWE to non-invasively predict the quality of VHR. Although further human studies are necessary, this work supports PRP use to improve VHR outcomes and US-SWE potential for bedside non-invasive hernia characterization.

Keywords Shear wave elastography · Ultrasound · Ventral hernia repair · Platelet-rich plasma · Acellular dermal matrix · Hernia

Jeffrey L. Van Eps and Anuj Chaudhry contributed equally to this work.

✉ Raffaella Righetti
righetti@ece.tamu.edu

1 Department of Surgery, Houston Methodist Hospital, Houston, TX, USA

2 Center for Biomimetic Medicine, Houston Methodist Hospital Research Institute, Houston, TX, USA

3 Department of Electrical and Computer Engineering, Texas A&M University, College Station, TX 77843-3128, USA

4 Centro de Biotecnología FEMSA, Escuela de Ingeniería y Ciencias, Tecnológico de Monterrey, Monterrey, Nuevo León, Mexico

5 Department of Electrical and Computer Engineering, Texas A&M University, 309D Wisenbaker Engineering Research Center, College Station, TX 77843-3128, USA

Ventral hernia repair (VHR) is one of the most common operations performed in the world with over 300,000 procedures performed annually in the United States alone [1]. Mesh materials used for repair may be broadly categorized into three groups—permanent synthetic, purely bioprosthetic [mesh containing biologic-derived materials, i.e., acellular dermal matrices (ADM)], and hybrid (combination permanent and biosynthetic materials). No mesh type is completely free of potential complication. The permanence of synthetic polymeric materials traditionally used has the benefit of long-term mechanical integrity but these are susceptible to infection or erosion [2]. Bioprosthetic mesh materials typically display improved biocompatibility and there is potential for its use in infected fields, yet they are not free of mesh-based complications [3]. Aside from variable allograft harvest integrity and elevated cost, the primary drawback of bioprosthetics is reduced mechanical strength over time leading to high rates of eventration and hernia recurrence, particularly when used for bridging VHR [4–6]. Some newer materials such as bioresorbable poly-4-hydroxybutyrate mesh (Phasix™, Bard Medical, New Providence, NJ, USA) and hybrid mesh have shown early clinical promise in high-risk patients but were not studied here and are beyond the scope of this discussion [7, 8].

In its most simplistic definition, platelet-rich plasma (PRP) is a plasma product derived from whole blood with a platelet concentration above baseline, known to contain a host of bioactive proteins, chemokines and growth factors within alpha granules that are released upon platelet activation [9, 10]. In use since the 1980s, PRP has shown efficacy in a variety of clinical applications including plastic surgery [11], bone regeneration [12], orthopedic and trauma surgery [13], and musculoskeletal injuries [14]. Though seemingly uniquely suited for soft tissue reconstruction, use of PRP in surgical treatment of soft tissue disease such as hernia repair has lagged behind and research evidence is conspicuously lacking. Our group has used animate models of soft tissue wound healing and abdominal reconstruction extensively to investigate ADM bioprosthetics and the ability of PRP to augment the native tissue response when used in VHR [6, 15–17]. Collectively, these results suggest that PRP may serve as a beneficial adjunct to improve VHR outcomes.

Monitoring patients for complication postoperatively after VHR is typically limited to bedside physical exam, traditional ultrasonography, or costly computed tomography (CT) or magnetic resonance (MR) imaging; and no current modality exists to qualitatively assess hernia repair with regards to prosthetic integrity and tissue incorporation. Ultrasound shear wave elastography (US-SWE) is a non-invasive imaging technique based on the speed of shear waves propagating through a tissue using real-time ultrasound (US) acquisition systems [18]. The shear wave velocity is then mapped into Young's modulus values by assuming the tissue to be an incompressible, single phase solid [19]. The Young's modulus essentially provides a quantitative measure of a tissue's mechanical stiffness. US-SWE has been used in a number of previous clinical applications, most notably the detection of liver fibrosis and cancers of the breast, prostate and thyroid [20–24]. In a previous study, we demonstrated the capability of US-SWE to image chronic ventral hernias pre- and post-repair using both synthetic and biologic meshes [25]. The results of this study demonstrated that synthetic mesh and porcine acellular dermal matrix (pADM) possess different mechanical properties (i.e., stiffness) that can be reliably detected and imaged non-invasively in vivo using US-SWE, establishing its potential as a useful future clinical modality to both diagnose ventral hernias and follow the integrity/incorporation of implanted meshes over time.

Prior work has established that the addition of PRP in VHR using pADM promotes early neovessel formation and increases tissue deposition, leading to overall better mesh incorporation and diminished hernia recurrence [15]. However, it is less clear how the use of PRP affects the mechanical properties at the site of VHR. Existing studies have shown that the stability and integrity of VHR indirectly correlates with the stiffness of the repair [26, 27]. However, a current lack of clinical modalities suitable for in vivo VHR mechanical assessment and a lack of in vivo data are found upon review of the literature. Bearing this in mind, our acting hypotheses in the following study are as follows: PRP treatment will improve non-invasive mechanical metrics of VHR using non-crosslinked pADM as assessed by Young's modulus, these mechanical changes can be non-invasively quantified in vivo by US-SWE, and correlate with quality of VHR as assessed by hernia recurrence and/or histologic parameters.

Materials and methods

Animal experiments: study design

Twenty-eight male Lewis rats (Charles River Labs, Houston, TX, USA) weighing 250–300 g were divided into two groups ($n = 14$) to undergo chronic VHR with Strattice™ (LifeCell Corporation, NJ, USA) non-crosslinked pADM either alone as a market control or augmented with autologous PRP. All animals were housed at the Houston Methodist Hospital Research Institute animal facility in pairs for a minimum acclimation time of at least 48 h until the time of ventral hernia creation (VHC), after which time they were housed individually. After VHC, all animals were monitored for a 28-day (minimum) incubation period in order to allow the hernia defect to mature and become chronic by definition. Rats were fed ad libitum and monitored daily for weight loss or surgical complication for the first five post-operative days,

followed by weekly assessment for 3 weeks until undergoing VHR. Similar procedure was followed after VHR until animal sacrifice at the assigned study endpoint. US-SWE analysis was performed before animal sacrifice at either three ($n = 8$/group) or six ($n = 6$/group) months after VHR. Animals were humanely euthanized using carbon dioxide gas followed by confirmatory thoracotomy prior to specimen harvest.

PRP isolation and characterization

Whole blood from ten donor Lewis rats was obtained for PRP isolation. After induction, inhalational anesthesia was maintained using 2.50–3.0% isoflurane via nosecone. Using aseptic techniques, a sternotomy was made and the heart exposed. A terminal cardiac blood draw was performed using a 22-gauge needle, and the blood admixed with 10% acid citrate dextrose to prevent clotting. This whole blood was centrifuged at 200×*g* for 15 min to facilitate removal of the red cell fraction (Fig. 1A). The remaining plasma portion was then centrifuged at 1600×*g* for 10 min to effectively pellet the remaining platelets. The plasma supernatant was then removed, leaving 1-mL total volume in which to redistribute the platelet pellet. The platelet number was quantified using a Multisizer Coulter Counter (Beckman Coulter, Pasadena, CA, USA) and plasma added or removed in order to generate a standardized final concentration of 1×10^6 platelets/μL of plasma. To confirm the final concentration, a complete blood cell count was performed on all final specimens. The PRP was then stored at − 80 °C.

Ventral hernia creation

The Institutional Animal Care and Use Committee (IACUC) at Houston Methodist Hospital Research Institute approved the proposed study, trained veterinary professionals monitored and participated in all phases of animal care, and all investigators complied with the National Research Council's *Guide for the Care and Use of Laboratory Animals*. All animals received pre-operative analgesia (Carprofen 5 mg/kg, and Buprenorphine 0.1 mg/kg) 30 min prior to surgery and for a minimum of 3 days postoperatively. Under the effects of inhalational anesthesia (2.5–3.0% isoflurane/O_2 gas mixture via nosecone) and in supine position, the abdominal fur was clipped and the operative site prepped with alternating scrubs of 2% chlorhexadine acetate solution and alcohol.

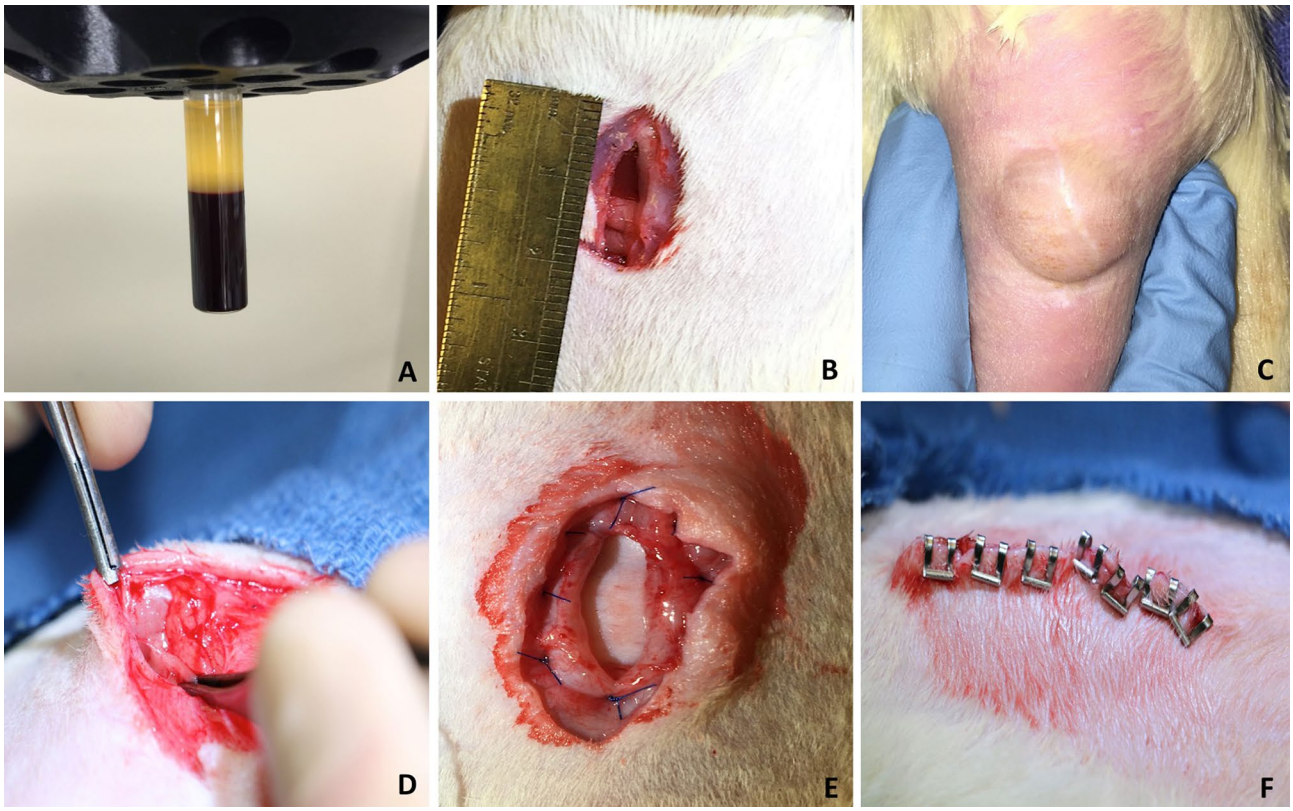

Fig. 1 Surgical procedure. Appearance of PRP after double-centrifugation technique (**A**). Ventral hernia defect creation (**B**). Representative appearance of ventral hernia 30 days after creation by incising abdominal wall (**C**). Dissection of ventral hernia and sac from surrounding tissues prior to mesh implantation (**D**). Secured pADM mesh bridging VHR (**E**). Completed VHR with surgical clip skin closure (**F**)

Aseptic technique was strictly maintained throughout. A 3 cm skin incision was made and skin flaps were raised in the avascular pre-muscular plane. This was followed by a full-thickness 2 cm vertical incision through the abdominal wall, entering the peritoneal cavity at the linea alba to create a midline hernia defect (Fig. 1B). Finally, the superficial skin and subcutaneous tissues were closed using wound clips. Elizabethan style exclusion collars (Kent Scientific, Torrington, CT, USA) were applied postoperatively to prevent incisional chewing for the first 4 days postoperatively after both VHC and VHR operations. Newly created hernias were allowed to mature for at least 4 weeks prior to subsequent VHR (Fig. 1C). Animals experiencing more than a 10% weight loss were treated with saline injections and moist pellets. Wound clips were removed on post-operative day 10–14.

Ventral hernia repair

After at least 28 days, rats underwent VHR. The prior incision site was entered and skin flaps were raised once again circumferentially. A combination of sharp dissection and sparing monopolar electrosurgical energy was utilized to excise the hernia sac and define the hernia borders (Fig. 1D). A 2.5–3.0 cm (diameter) piece of Strattice™ mesh was hydrated according to manufacturer instructions and customized to the shape of the fascial defect to allow for at least 5 mm of overlap between the native abdominal wall muscle and mesh. A bridging intraperitoneal onlay mesh (IPOM) repair was performed, with the bioprosthetic mesh secured using eight interrupted, transabdominal 5-0 Prolene (Ethicon, Somerville, NJ, USA) sutures placed at equal intervals (Fig. 1E). Prior to fixation, the anterior surface of each mesh was soaked for 5 min in either 200 µL of saline (controls) or 200 µL of PRP (experimental group) activated with bovine thrombin (5000 units, Sigma-Aldrich, St. Louis, MO, USA) with the remainder applied to the anterior surface just before closure. Although typically approximated in human procedures, the tissue defect overlying mesh was intentionally not closed in order to maximize in vivo strain on the pADM implant and help uncover differences in outcomes between experimental groups. Also, since the effect of a rodent milieu on material longevity was not known, permanent rather than absorbable suture was chosen in order to avoid any complications related to suture degradation. The skin was closed with wound clips and post-operative care was undertaken in identical fashion to that previously described after VHC (Fig. 1F).

Ultrasound shear wave elastography (US-SWE)

To remove abdominal wall motion variability that naturally occurs with the respiratory cycle, US-SWE was performed immediately post-mortem. The technique used was identical to that outlined in our original work [25]. Specifically the rats were imaged with an Aixplorer®, Supersonic Imagine (Aix-en-Provence, France) US machine using a 3.5 MHz probe (SC6-1, SuperSonic Imagine) in penetration mode (lower frequency/resolution setting). The depth of acquisition was standardized to 2 cm. Young's modulus (E) measurements were obtained by choosing a 1 mm^2 circular ROI (Q-box™) at the implant region. Elastography data from experimental PRP-treated rats were then statistically compared with control cases. A paired *t* test was used with 95% confidence interval.

Histological analysis

H&E staining

To assess tissue architecture, explanted specimens were embedded in paraffin, microtome sectioned into 7 µm-thick slices, and stained using the following standard hematoxylin and eosin (H&E) staining protocol: slides were submerged in 100% xylene three times, then transferred in a stepwise fashion from 50:50 xylene/100% Ethanol to 100%, 95%, to distilled water. Samples were then placed in Gill´s hematoxylin (Sigma-Aldrich, St. Louis, MO, USA), rinsed under tap water, briefly submersed in acid alcohol, and washed in tap water again before being placed in ammonia water solution 0.2% followed by a final tap water rinse. Next, samples were stained in eosin Y (Sigma-Aldrich) for one minute and washed with tap water before taking them through timed submersion in ethanol baths of successively increasing concentrations. Finally, slides were mounted using cytoseal XYL (Thermo Scientific, Waltham, MA, USA).

Semi-quantitative histologic scoring

Images from H&E stained 3-month sample slides were analyzed to generate a quantitative score as previously reported by Brown et al. [28]. Images were taken at ×40 magnification using an EVOS FL Auto Cell Imaging System at multiple locations along the mesh-tissue interface. Samples from both groups had at least four images analyzed by a single blinded observer trained in histopathology for the following parameters on a scale from 0 to 3: presence of multinucleated giant cells, connective tissue organization, muscle ingrowth, encapsulation, and scaffold degradation (Table 1). Scores from both groups were averaged for statistical comparison using Graphpad Prism software (La Jolla, CA, USA). To assess significance an unpaired Student's *t* test was used with an alpha established at 0.05.

Table 1 Semi-quantitative histologic scoring. Reproduced with permission from Brown et al. [28]. Copyright 2012 by Elsevier

	0	1	2	3
Multinucleated giant cells (# per 40× field)	> 5	2–5	1	0
Connective tissue organization	Original scaffold intact	Scaffold disrupted, poorly organized new ECM present	Moderately organized connective tissue present	Dense, highly organized connective tissue present
Muscle ingrowth	None	Muscle cells present at periphery	Muscle cells present in center	Organized muscle present
Encapsulation	Dense tissue encapsulation	Moderate encapsulation	Slight encapsulation	None
Degradation	Scaffold completely intact	Scaffold mostly present	Some scaffold present	No scaffold present

Results

Animal surgery outcome

All rats had hernias successfully created but with variable subsequent protrusion of intra-abdominal contents. After VHR, rates of seroma formation were not statistically different between the groups with 6 PRP (−) rats and 5 PRP (+) rats forming seroma. However, none of these became clinically significant with signs of infection or otherwise requiring drainage, animal sacrifice, or other intervention. Also, no animals suffered surgical site infection separate from the presence of seroma. Some animals in each group had significant weight loss in the early post-operative period (defined as > 5% decrease in weight from baseline) but there was no statistical difference between the groups, with 5 PRP (−) rats and 4 PRP (+) rats suffering weight loss. At the 3-month time point, PRP (+) rats demonstrated greater gross neovascularization of implanted mesh on average than PRP (−) rats and this was supported at the microscopic level on histologic analysis. At the 6-month time point the differences were striking, with 67% (4/6 animals) of PRP (−) animals suffering gross hernia recurrence from central mesh failure as opposed to zero mesh failures in the PRP-treated group. The remaining 2 PRP (−) rats had an extremely thin remaining mesh implant that would have undoubtedly failed over time. PRP-treated rats had greatly preserved implant thickness comparatively.

Ultrasound shear wave elastography (US-SWE)

Similar to our previous study [25], the mesh was consistently, reliably distinguished from surrounding native tissues as a region of higher stiffness in the respective elastograms from both PRP-treated and control rats at the 3-month time point (Fig. 2). US-SWE demonstrated 100% sensitivity in detecting hernia recurrence by visualized colorimetric differences in stiffness surrounding the fascial defect and was consistently confirmed at the time of completion of animal sacrifice and abdominal wall harvest.

The estimated Young's modulus generated by US-SWE was invariably higher in the PRP-treated group at both time points. The mean Young's modulus of the PRP (+) group was 38.1 ± 3.7 and 44.6 ± 3.1 kPa, while the control group averaged 21.5 ± 1.4 and 17.6 ± 4 KPa at the 3-month and 6-month time points respectively ($p < 0.05$, Fig. 3). The Young's modulus of the expected mesh region in cases of hernia recurrence averaged 4.4 ± 1.6 kPa.

Qualitative histomorphological analysis

Histological comparison of 6-month samples was precluded by the high incidence of mesh failure in the control group. The remaining control samples at this time point without gross recurrence were so thin that they suffered iatrogenic mesh failure simply during harvesting and histological processing. However, images taken at the interface between native abdominal wall tissue and mesh implant show a pronounced difference between control samples and those enriched with PRP at 3 months. Qualitative analysis of control samples reveals a preservation of overall tissue structure, and the presence of collagen deposition atop the mesh implant but in a less organized fashion compared to PRP-treated samples. Additionally, there is significantly increased hematoxylin-stained cellularity on the inside border of the mesh implant and at the mesh-abdominal wall interface (Fig. 4 A, B), consistent with a chronic (lymphocytic) infiltrate. The collection of immune cells here including macrophages and foreign body giant cells (FBGCs), along with the apparent encapsulation seen around the implant, connote a possible adverse foreign body reaction in PRP (−) samples. Histological analysis of a similar group of animals implanted with PRP (+) mesh displayed no altered macro structure of anatomical features, a conspicuous absence of hematoxylin-laden cells, and signs of incorporation rather than encapsulation (Fig. 4 C, D). For example, the deposited tissue is more organized with superior mimicry of biologically active native tissue, demonstrated by the enhanced presence of neovessels and even myofibroblast cell islands at the interface.

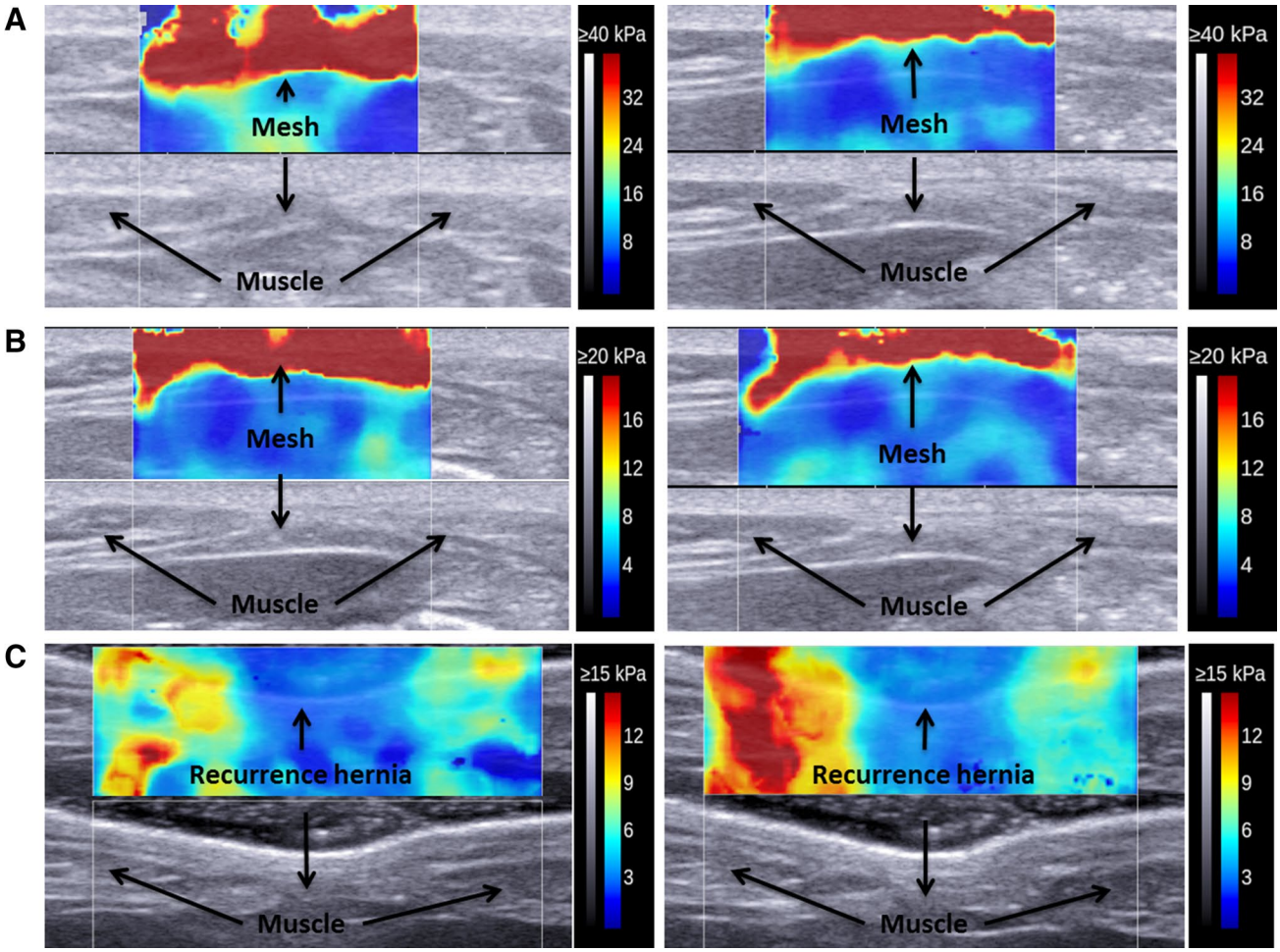

Fig. 2 US elastography. Representative US-SWE images from cases of: **A** PRP-treated, **B** control and **C** hernia recurrence

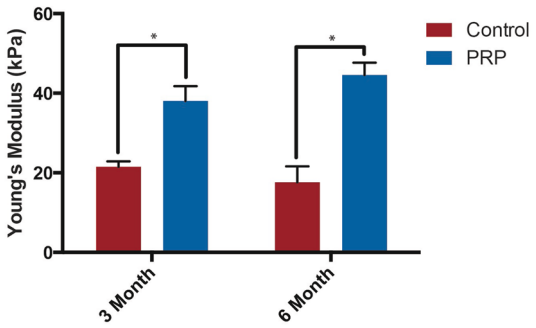

Fig. 3 Young's modulus. Mean and standard deviation of Young's modulus estimated from US-SWE at 3 and 6 months postoperatively for PRP-treated versus control VHR. $*p < 0.05$

Semi-quantitative histomorphological analysis

To add objective, quantitative representation of the histologic phenomena listed above, semi-quantitative analysis of sample slides was performed. Control specimens displayed more severe encapsulation and diminished muscle ingrowth compared with PRP-treated specimens. Also, although most of the scaffold was still present, there were areas of inflammatory cell infiltration where degradation was appearing, whereas this was not witnessed in PRP-treated samples. No statistically significant difference was witnessed in giant cell macrophages between groups. Collectively, this resulted in a significantly higher mean score in the experimental group receiving PRP ($p = 0.012$). Together these results show that PRP-treated samples show better incorporation into surrounding tissue with less signs of rejection and could be correlated with a better prognosis for hernia repair operations that incorporate PRP.

Discussion

VHR remains a popular topic of surgical research due both to its impact on public health as one of the most commonly performed procedures, and the opportunities for

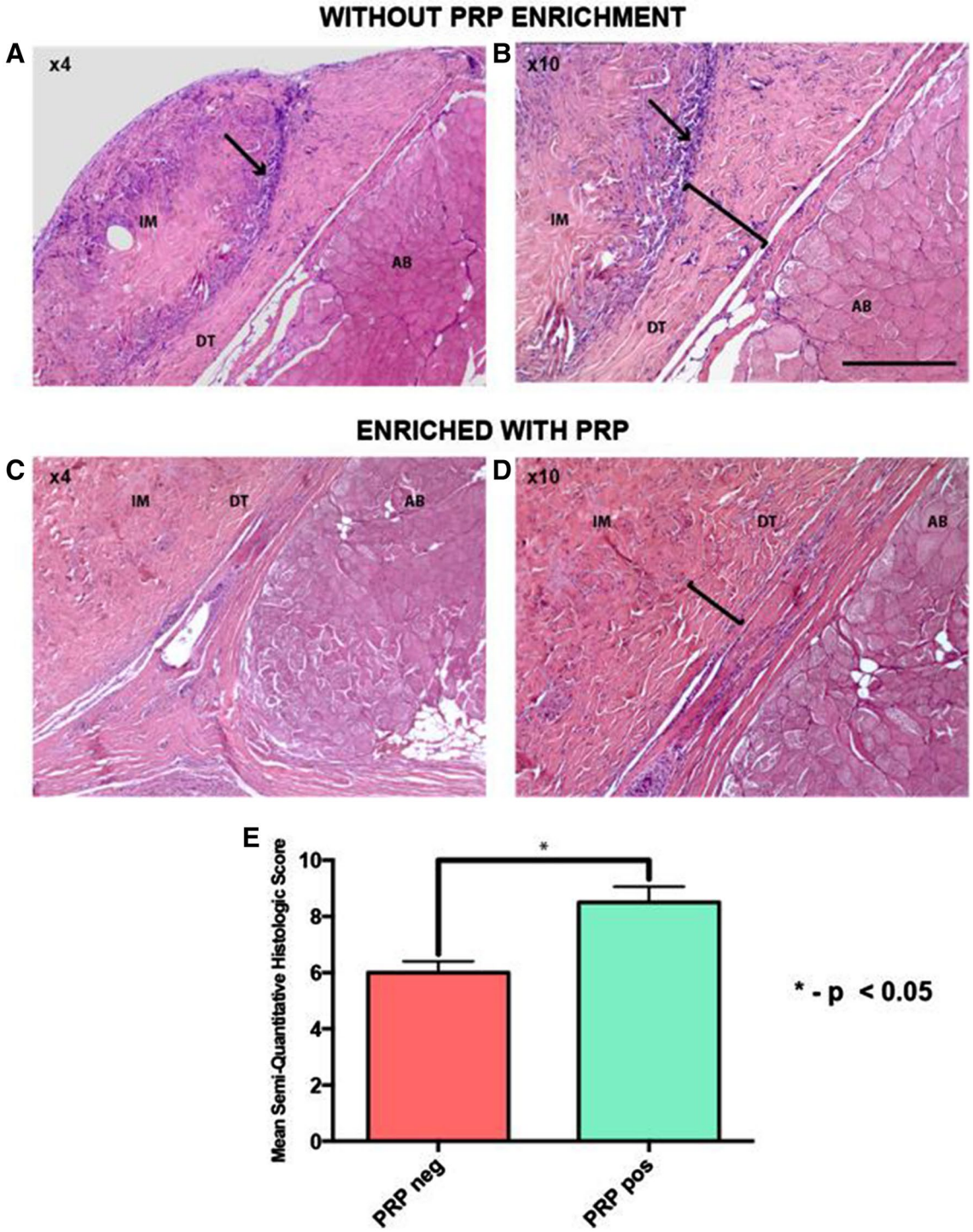

Fig. 4 Qualitative and semi-quantitative histological analysis: control samples show pronounced cellular infiltration present on inside border of the implant, indicating signs of chronic inflammation as well as less organized tissue deposition with some encapsulation (bracketed), as captured at ×4 magnification (**A**) and ×10 magnification (**B**) light microscopy. The interface of PRP-treated meshes showed no signs of increased infiltration and a more contiguous, coordinated collagen fibril deposition with enhanced neovascularization and myofibroblast islands, again visualized at ×4 and ×10 (**C, D**). Graphical representation of comparative histological semi-quantitative analysis confirming superiority of PRP-treated samples (**E**, $*p < 0.05$). Scale bar 0.5 mm, *IM* implanted mesh, *DT* deposited tissue, *AB* abdominal wall

improvement both in mesh implants and surgical technique utilized. Each class of implantable mesh available has individualized benefits and limitations. Synthetic matrices provide excellent mechanical integrity but at the cost of infection risk, increased visceral adhesions, and implant permanence. Although ADMs display improved biocompatibility compared to their synthetic counterparts, their use in VHR has been limited due to prohibitive cost and long-term mechanical weakening that ultimately results in high rates of hernia recurrence. Existing literature shows that hernia recurrence plagues hernia repair of every type, with recurrence rates greater than 30% at 10 years post-repair [29]. Logically, the addition of exogenous biologic moieties such as growth factors to VHR could theoretically augment the regenerative host response to implanted bioprosthetics. Although noteworthy progress has been made in controlled-release applications of protein payloads, including recent work from our own lab, clinical use of this technology with synthetic exogenous growth factors introduces several obstacles, including: biostability and space constraints during storage, scalability, biocompatibility, and prohibitive cost [30–34]. The ideal alternative would be an autologous product that is easily processed and applied clinically, and provides similar biologic activity to exogenous sources. PRP embodies all of these desirable characteristics and has been shown by others to be widely efficacious in enhancing soft tissue healing broadly, and enhancing VHR specifically by our study group. However, diagnosis and follow up for patients after VHR remains a challenge.

Due to a host of factors limiting the efficacy of bedside clinical examination, including body habitus and varied size or anatomy of ventral hernias, clinicians are left largely with imaging modalities such as CT or MRI to assess recurrence. These tests have many drawbacks such as cost and radiation exposure. Bedside 2-dimensional US may be effective to document the presence of a hernia but gives no indication as to the quality of tissue healing or incorporation at the site of VHR after surgery. The availability of a safe bedside imaging modality that can not only diagnose a hernia or its recurrence, but also give data regarding the integrity of VHR to be followed over time could effectively revolutionize hernia surgery. We have previously demonstrated the ability of US-SWE to reliably provide 2D and 3D imaging at the site of an existing hernia as well as the individual components (mesh, native abdominal wall) after VHR [25]. The aim of the current study was to investigate the ability of US-SWE to go beyond imaging and provide quantitative/qualitative assessment of VHR, meanwhile investigating the ability of PRP to improve the outcomes of VHR at both the macroscopic and microscopic levels.

Evidence of PRP's beneficial effect was witnessed at both the gross and histologic level. Compared to controls at 3 months, PRP-treated samples invariably showed enhanced neovascularization, decreased chronic inflammatory cell infiltrates, and more active cellular migration and regeneration at the interface of native tissue with mesh implant to signify incorporation as opposed to encapsulation. Such effects are likely secondary to the bioactive scaffolding provided by PRP application to the mesh interface, which promotes cellular migration and retention. These tissue effects, along with protection from immunologic degradative thinning of the ADM implant translated into enhanced physical integrity at the mesh-tissue interface and total protection from hernia recurrence at 6 months in PRP-treated animals. This effect was pronounced when compared to the majority of control animals that suffered such a complication, and suggests that the effect of simplistic PRP addition at the time of surgery is not limited to the short post-operative period after VHR, but rather has far-reaching long-term sequelae. We believe such effects to be primarily rooted in immunologic cellular guidance toward a pro-regenerative rather than pro-inflammatory response, but this requires further study which we are currently undertaking. Interestingly, these significant differences at the microscopic level were effectively predicted by our *ex vivo* US-SWE analysis.

Our prior work confirmed the ability of US-SWE as a bedside tool to characterize an existing hernia before or after repair with mesh in 2D and 3D [25]. Data from our current study show that US-SWE analysis reliably predicts differences in healed tissue quality and ADM integrity. Animals treated with PRP demonstrated a Young's modulus 1.78 and 2.54 times higher than the control group at 3 and 6-month time points respectively with narrow standard deviations. Subsequent histological processing showed that this difference in *ex vivo* 'stiffness' reflects very important disparities in classic metrics of ADM biocompatibility and host incorporation. US-SWE also showed reliability in diagnosing hernia recurrence using Young's modulus as well, with values observed at the VHR site in cases of recurrence (4.4 ± 1.6) that were statistically similar to those witnessed in the case of unrepaired ventral hernias (2.9 ± 0.6) in previous studies [25].

This study had several limitations. Though we would have preferred to use larger experimental groups, the financial burden of operating on additional rats and providing care for them for such prolonged post-operative time points was cost-prohibitive. Our prior work with PRP augmentation of VHR has demonstrated large differences in outcomes of interest, allowing for adequately powered studies with smaller study groups. Our goal remains to perform operative studies that induce pain in the smallest number of animal subjects to gather the necessary data and we were fortunate to witness striking, consistent differences in our treatment groups reaching statistical significance. The uniformity of mesh thinning or failure in the control group provided prominent evidence of treatment difference between groups but

did limit our histologic comparison of the central mesh area. Molecular evidence would have provided useful corroboration of the stated findings but was viewed as less important at such remote time points from the index operation, and the early post-operative time points of interest molecularly have previously been characterized by our group [6, 15, 16].

Although further investigation is needed in human subjects, together with our prior work, this study implies that US-SWE carries potential as a possible future adjunct for the herniologist not only to characterize existing ventral hernias, but also to monitor patients postoperatively for the quality/integrity of healing at the site of VHR; and potentially even stratify patients at risk for hernia recurrence all at the outpatient bedside using real-time, in-office, technology. Although this is perhaps more of a testament to the glaring current shortcomings of available technologies for hernia characterization, the availability of this technology would certainly represent a true leap forward in the clinical care of hernia patients. Collectively, this work purports the use of PRP and US-SWE as effective clinical additions in the diagnosis, characterization, and treatment of ventral hernias with implantable materials, but requires further study in the form of human trials.

Conclusion

This study provides further confirmation of PRP's ability to enrich the integrity of VHR using ADM, and proof of concept data that the quality of such VHR can be reliably predicted using US-SWE imaging. The findings reported using US-SWE and histological assessment independently confirm the advantage of PRP supplementation in VHR. The addition of PRP increased tissue integrity at the ADM–host interface by establishing a pro-regenerative milieu while diminishing immunologic mesh degradation, ultimately protecting from hernia recurrence. The addition of a low-cost, autologous material that improves the integrity and acceptance of implants in hernia repair surgery could have substantial impact in the reduction of morbidity associated with this procedure and a significant effect on public health. Meanwhile, the implementation of US-SWE into clinical practice may possibly improve care by providing the herniologist with a real-time, radiation-free modality to characterize the repaired and unrepaired hernia in the outpatient setting.

Funding This work was supported by external funding from The Cullen Trust for Health Care, Cancer Prevention & Research Institute of Texas (Award ID RP170466).

Compliance with ethical standards

Disclosures Jeffrey L. Van Eps, Anuj Chaudhry, Joseph S. Fernandez-Moure, Christian Boada, Vishwanath Chegireddy, Fernando J. Cabrera, Songyuan Tang, Ennio Tasciotti, and Raffaella Righetti; nor their close family members, have no conflict of interest or financial ties to disclose.

References

1. Poulose BK et al (2012) Epidemiology and cost of ventral hernia repair: making the case for hernia research. Hernia 16(2):179–183
2. Falagas M, Kasiakou S (2005) Mesh-related infections after hernia repair surgery. Clin Microbiol Infect 11(1):3–8
3. Breuing K et al (2010) Incisional ventral hernias: review of the literature and recommendations regarding the grading and technique of repair. Surgery 148(3):544–558
4. Blatnik J, Jin J, Rosen M (2008) Abdominal hernia repair with bridging acellular dermal matrix—an expensive hernia sac. Am J Surg 196(1):47–50
5. Zhang J et al (2011) The biomechanical behavior and host response to porcine-derived small intestine submucosa, pericardium and dermal matrix acellular grafts in a rat abdominal defect model. Biomaterials 32(29):7086–7095
6. Van Eps J et al (2016) Decreased hernia recurrence using autologous platelet-rich plasma (PRP) with Strattice mesh in a rodent ventral hernia model. Surg Endosc 30(8):3239–3249
7. Bittner JGt et al (2018) First human use of hybrid synthetic/biologic mesh in ventral hernia repair: a multicenter trial. Surg Endosc 32(3):1123–1130
8. Buell JF et al (2017) Initial experience with biologic polymer scaffold (poly-4-hydroxybuturate) in complex abdominal wall reconstruction. Ann Surg 266(1):185–188
9. Foster TE et al (2009) Platelet-rich plasma from basic science to clinical applications. Am J Sports Med 37(11):2259–2272
10. Fernandez-Moure JS et al (2017) Platelet-rich plasma: a biomimetic approach to enhancement of surgical wound healing. J Surg Res 207:33–44
11. Eppley BL, Pietrzak WS, Blanton M (2006) Platelet-rich plasma: a review of biology and applications in plastic surgery. Plastic Reconstr Surg 118(6):147e–159e
12. Griffin X, Smith C, Costa M (2009) The clinical use of platelet-rich plasma in the promotion of bone healing: a systematic review. Injury 40(2):158–162
13. Alsousou J et al (2009) The biology of platelet-rich plasma and its application in trauma and orthopaedic surgery a review of the literature. J Bone Joint Surg Br 91(8):987–996
14. Sampson S, Gerhardt M, Mandelbaum B (2008) Platelet rich plasma injection grafts for musculoskeletal injuries: a review. Curr Rev Musculoskelet Med 1(3–4):165–174
15. Fernandez-Moure JS et al (2015) Platelet rich plasma enhances tissue incorporation of biologic mesh. J Surg Res 199(2):412–419
16. Fernandez-Moure JS et al (2016) Porcine acellular lung matrix for wound healing and abdominal wall reconstruction: a pilot study. J Tissue Eng 7:2041731415626018
17. Minardi S et al (2017) Biomimetic collagen/elastin meshes for ventral hernia repair in a rat model. Acta Biomater 50:165–177
18. Bercoff J, Tanter M, Fink M (2004) Supersonic shear imaging: a new technique for soft tissue elasticity mapping. IEEE Trans Ultrason Ferroelectr Freq Control 51(4):396–409
19. Sarvazyan AP et al (1998) Shear wave elasticity imaging: a new ultrasonic technology of medical diagnostics. Ultrasound Med Biol 24(9):1419–1435
20. Chang J et al (2011) Clinical application of shear wave elastography (SWE) in the diagnosis of benign and malignant breast diseases. Breast Cancer Res Treat 129(1):89–97

21. Doyley MM (2012) Model-based elastography: a survey of approaches to the inverse elasticity problem. Phys Med Biol 57(3):R35
22. Barr RG, Memo R, Schaub CR (2012) Shear wave ultrasound elastography of the prostate: initial results. Ultrasound Q 28(1):13–20
23. Evans A et al (2012) Invasive breast cancer: relationship between shear-wave elastographic findings and histologic prognostic factors. Radiology 263(3):673–677
24. Lyshchik A et al (2005) Thyroid gland tumor diagnosis at US elastography 1. Radiology 237(1):202–211
25. Chaudhry A et al (2017) Characterization of ventral incisional hernia and repair using shear wave elastography. J Surg Res 210:244–252
26. Burger J et al (2006) Evaluation of new prosthetic meshes for ventral hernia repair. Surg Endosc Other Interv Tech 20(8):1320–1325
27. Jenkins SD et al (1983) A comparison of prosthetic materials used to repair abdominal wall defects. Surgery 94(2):392–398
28. Brown BN et al (2012) Macrophage phenotype as a predictor of constructive remodeling following the implantation of biologically derived surgical mesh materials. Acta Biomater 8(3):978–987
29. Burger JWA et al (2004) Long-term follow-up of a randomized controlled trial of suture versus mesh repair of incisional hernia. Ann Surg 240(4):578
30. Anitua E et al (2008) Delivering growth factors for therapeutics. Trends Pharmacol Sci 29(1):37–41
31. Chiappini C et al (2015) Biodegradable nanoneedles for localized delivery of nanoparticles in vivo: exploring the biointerface. ACS Nano 9(5):5500–5509
32. Martinez JO et al (2012) Multifunctional to multistage delivery systems: the evolution of nanoparticles for biomedical applications. Chin Sci Bull 57(31):3961–3971
33. Minardi S et al (2015) PLGA-mesoporous silicon microspheres for the in vivo controlled temporospatial delivery of proteins. ACS Appl Mater Interfaces 7(30):16364–16373
34. Murphy MB et al (2011) Multi-composite bioactive osteogenic sponges featuring mesenchymal stem cells, platelet-rich plasma, nanoporous silicon enclosures, and Peptide amphiphiles for rapid bone regeneration. J Funct Biomater 2(2):39–66